Post-warming re-expansion and contraction dynamics of vitrified blastocysts: shrinkage magnitude and timing are correlated with pregnancy outcome

Laura Conversa, M.Sc.,[a] Carla Giménez-Rodríguez, M.Sc.,[a] Lucía Murria, M.Sc.,[a] Lucía Alegre, M.Sc.,[b] Ana Cobo, Ph.D.,[a,b] and Marcos Meseguer, Ph.D.[a,b]

[a] IVIRMA Global Research Alliance-IVI Foundation, Health Research Institute La Fe, Reproductive Medicine, Valencia, Spain; [b] IVIRMA Global Research Alliance-IVI Valencia, IVF Laboratory, Valencia, Spain

Objective: To analyze the relationship between blastocyst postwarming dynamics, specifically re-expansion and contractions, with implantation and live birth (LB) rates and overall embryo viability after vitrification and warming.
Design: Retrospective cohort study.
Setting: University-affiliated private in vitro fertilization center.
Subjects: A total of 846 warmed blastocysts from patients undergoing frozen cycles (February 2022 to May 2024).
Intervention: None.
Main Outcome Measures: Postwarming re-expansion dynamics and contraction types—pre–re-expansion contractions (PRCs) and mid–re-expansion contractions (MRCs) (pumping or collapsing)—inner cell mass size, and cytoplasmic strings (CSs) were analyzed for their correlation with implantation and LB rates. Additionally, logistic regression models incorporated these variables alongside conventional and artificial intelligence (AI)–based embryo quality assessments.
Results: Of the 846 vitrified blastocysts, 97.5% survived warming, of which 95.5% were able to initiate re-expansion. Implantation and LB rates were higher (46.8% and 46.9%, respectively) in re-expanded vs. non–re-expanded blastocysts (18.2% for both outcomes). Faster re-expansion speed, thinner zona pellucida, larger final blastocyst size, and larger inner cell mass area were positively correlated with successful treatment outcomes. Moreover, CSs were identified in 47.4% of embryos and associated with implantation (50.5% vs. 43%). The presence of PRCs was associated with higher implantation rates (50% vs. 42.1%). In contrast, the presence of collapse (MRC shrinkage, >15%) reduced implantation (from 47.3% to 31.8%) and LB (from 41.5% to 27.3%) rates. Pumping (MRC shrinkage, <15%) embryos were more likely to hatch naturally after warming (18.8% vs. 8.7%). Postwarming contractions were correlated with embryo morphological quality assessed by embryologists and an image-based AI software.
Conclusion: Postwarming re-expansion and contraction dynamics are critical indicators of embryo viability and competence. Specifically, strong MRCs or collapses negatively affect implantation and LB potential, whereas minor contractions or pumping may assist in successful hatching. Faster re-expansion, PRC presence, and CS improve implantation outcome, suggesting a need to take these data into account when evaluating warmed embryos and to integrate contraction metrics into AI-assisted embryo selection. Thus, enhanced monitoring of these dynamics may guide embryo selection and clinical decision-making, ultimately optimizing pregnancy success rates. (Fertil Steril® 2026;125:640–9. ©2026 by American Society for Reproductive Medicine.)
El resumen está disponible en Español al final del artículo.

Key Words: Vitrification, blastocyst, re-expansion, spontaneous collapse, time-lapse imaging

Received April 11, 2025; revised October 6, 2025; accepted October 7, 2025; published online October 14, 2025.
Supported by a grant from the Regional Ministry of Innovation, Universities, Science and Digital Society of the Valencian Community (Valencia, Spain) (CIACIF/2021/019), and by Spanish Ministry of Science and Innovation (Madrid, Spain) (CDTI-IDI-20240634).
Data regarding any of the subjects in the study has not been previously published unless specified. Data will be made available to the editors of the journal for review or query upon request.
The data underlying this article will be shared upon reasonable request to the corresponding author.
Correspondence: Marcos Meseguer, Ph.D. (E-mail: marcos.meseguer@ivirma.com).

Fertil Steril® Vol. 125, No. 4, April 2026 0015-0282/$36.00

https://doi.org/10.1016/j.fertnstert.2025.10.013

Since the first live birth (LB) from a frozen human embryo (1) and the introduction of vitrification (2), embryo cryopreservation has significantly advanced, improving the efficiency and success rates of assisted reproduction techniques. The widespread adoption of "freeze-all" and "single embryo transfer" strategies has contributed to a steady increase in vitrified cycle transfers (3).

Vitrification involves exposing the embryo to a highly concentrated cryoprotectant solution, replacing most intracellular and blastocoelic water and facilitating a glassy cytosolic state when immersed in liquid nitrogen. This process causes morphological changes because of blastocoel fluid loss. During warming, blastocysts rehydrate while releasing cryoprotectants (4) and are typically cultured for 3–5 hours to allow re-expansion before transfer (5). This re-expansion, the recovery of blastocoel volume, likely requires trophectoderm (TE) resealing to enable water retention, as also observed in porcine blastocysts after warming (6).

The mechanism of re-expansion is comparable to blastocoel expansion during fresh embryo development, with TE cells pumping sodium ions into the blastocoel, driving osmotic water influx via aquaporins (7, 8). Tight junctions connecting TE cells provide a barrier that allows fluid accumulation (9). Therefore, re-expansion reflects membrane permeability and osmotic capacity, both crucial for effective vitrification and warming.

Multiple studies confirm that early and extensive re-expansions are critical indicators of blastocyst viability (5, 10–16). It is also correlated with implantation potential by thinning the zona pellucida (ZP), facilitating hatching and endometrial contact.

However, re-expansion does not always occur or sometimes does not follow a linear pattern. Warmed blastocysts may undergo spontaneous contractions, which are partial or total detachments of the TE from the ZP. Blastocoel contraction was first reported in rabbit embryos by Lewis and Gregory (17) in 1929. Some studies suggest that weak contractions (<20% volume reduction) may promote hatching, whereas stronger ones (≥20%) inhibit it and reduces implantation potential because of energy imbalance (18, 19). Fresh collapses have also been linked to poor embryo quality, aneuploidy, and lower LB rates (20–22), although their predictive value is debated (23).

Most time-lapse studies on contraction have focused on fresh blastocysts, and it is unclear whether the underlying cause of this phenomenon is the same for vitrified-warmed blastocysts. However, evidence suggests that vitrification may increase the frequency of contractions during prehatching stage (24). These postwarming dynamics can be accurately monitored using time-lapse systems.

Maezawa et al. (25) proved that collapsed blastocysts consumed less oxygen than expanded ones; however, this did not reflect implantation. Other researchers used time-lapse to quantify warmed blastocyst morphology, such as the initial and final blastocyst area, inner cell mass (ICM) size, and presence of collapses, with the latter showing no correlation with outcomes, although methodological differences such as assisted hatching may have influenced results (14,15).

Existing studies do not differentiate between contractions occurring before re-expansion onset and those during the process itself. Our previous findings suggest that strong mid–re-expansion contractions (MRCs) negatively impact embryo viability, as reflected by lower artificial intelligence (AI) scores and implantation failure (26). Under these premises, we hypothesized that both the timing and degree of contraction after warming may influence embryo competence. Here, we retrospectively analyze different parameters of postwarming blastocyst dynamics and their relationship with survival to vitrification and clinical outcomes in a heterogeneous population, aiming to enhance the generalizability of our results.

MATERIALS AND METHODS

Study design and population

This retrospective analysis included 846 vitrified blastocysts warmed between February 2022 and May 2024 at IVI Valencia (Spain). The protocol for this study was approved by the Institutional Review Board (code 2111-VLC-104-MM) of the clinic. All embryos were incubated in EmbryoScope time-lapse systems between warming and either transfer (n = 820), discard because of nonviability (n = 21), or revitrification (n = 5). Revitrification was performed when an embryo failed to re-expand, warming up another one for transfer, or when the transfer was cancelled. Of the 820 embryos transferred, implantation data were available for 815, and LB data were available for 799.

Blastocyst lengths and diameters (Video 1, available online) involved in re-expansion and contractions, ICM

FIGURE 1

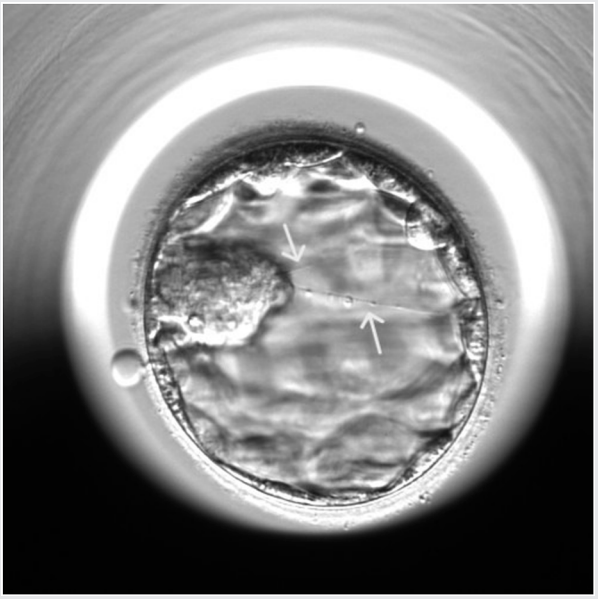

Cytoplasmic strings between the inner cell mass and the trophectoderm.

Conversa. Contractions of vitrified blastocysts. Fertil Steril 2026.

diameter, and cytoplasmic strings (CSs) were manually annotated using EmbryoViewer drawing tool (Vitrolife, Gothenburg, Sweden). Cytoplasmic strings are cytoplasmic connections between TE cells and ICM cells during the blastocyst stage (Fig. 1). Re-expansion parameters noted and calculated were the following: start/end time (hour); re-expansion duration (hour); ZP maximum/minimum thickness (μm); initial/final blastocyst size (μm^2); blastocyst size at the beginning/ending of re-expansion (μm^2); ZP thinning (μm); re-expansion size (μm^2); and speed (μm^2/h).

Contractions were analyzed on the basis of their number, shrinkage percentage (calculated as [{precontraction area−contraction area}/precontraction area] × 100) and timing (pre–re-expansion vs. mid–re-expansion). Pre–re-expansion contraction (PRC) occurred before re-expansion onset, whereas MRCs occurred once re-expansion had started (Fig. 2).

Artificial intelligence software *Embryo Assess* (Alife Health, San Francisco, California) retrospectively analyzed previtrification, first, and final postwarming images to assess the relationship between embryo quality, contractions, and outcomes. Some images were not scored because of technical issues. The algorithm was trained on images of fresh blastocysts on day 5/6/7 before transfer or cryopreservation (27).

Ovarian stimulation and oocyte retrieval

In autologous cycles, ovarian stimulation initiated with gonadotropins (follicle-stimulating hormone level, 150–300 IU/d) within the first 3 days of menstruation. A gonadotropin-releasing hormone (GnRH) antagonist was administered when a follicle reached 14 mm (28). When follicles reached 17–18 mm, final oocyte maturation was triggered with 0.2 mg of GnRH agonist and/or 250 mcg of recombinant hCG (Ovitrelle; Merck Serono, Saint-Aubin, Switzerland). In donor cycles, ovarian stimulation was performed using a GnRH agonist (Decapeptyl; Ipsen Pharma, Boulogne-Billancourt, France) until at least 8 follicles reached approximately 18 mm, and oocyte retrieval was scheduled 36 hours later. Recipients underwent endometrial preparation via hormone replacement therapy (29). Natural cycles were performed according to the routine practice of the clinic (30).

Fertilization and embryo culture

Denudation and fertilization via intracytoplasmic sperm injection were performed as in the study by Valera et al. (31). Fertilized oocytes were cultured individually in time-lapse incubators using single-step medium (Gems; Genea Biomedx, Sydney, Australia) and mineral oil (FertiCult; FertiPro, Beernem, Belgium). Fertilization was confirmed at 16–19 hours after intracytoplasmic sperm injection. Senior embryologists assessed blastocysts at days 5 and 6, following the Spanish Association for the Study of Reproductive Biology (ASEBIR) guidelines (32), on the basis of expansion, ICM and TE quality. Embryo selection followed ASEBIR's hierarchical classification (categories A, B, and C) and AI scoring (33).

Preimplantation genetic testing for aneuploidies

Embryos in the preimplantation genetic testing for aneuploidies (PGT-A) program (n = 140) were taken out of the incubator on day 3, and a laser-assisted hole was made in the ZP to create a small opening and facilitate hatching.

FIGURE 2

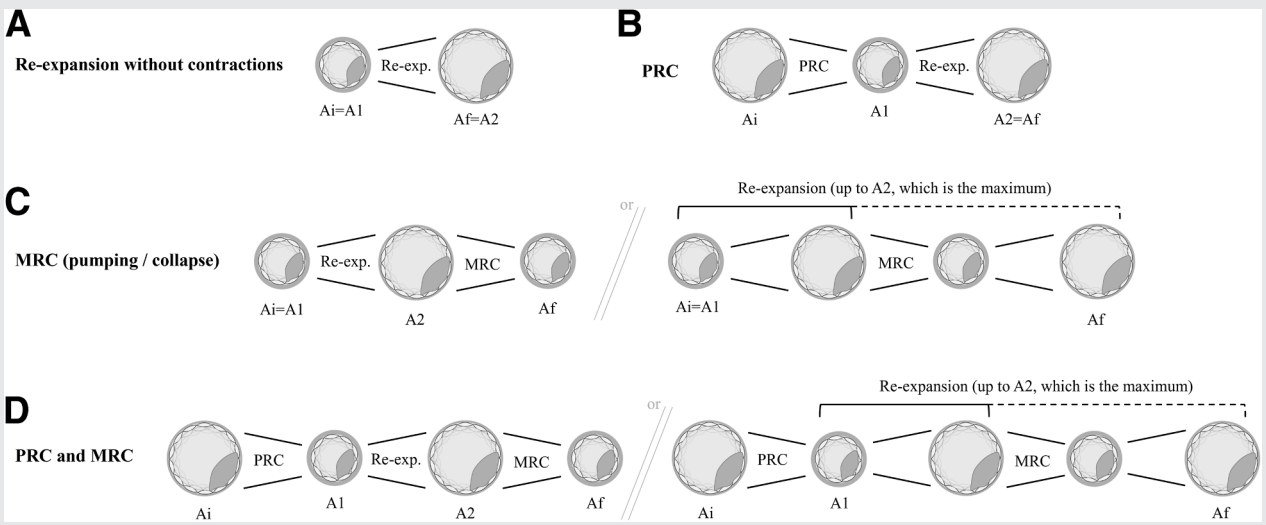

Types of postwarming re-expansion dynamics: re-expansion without contractions (**A**); pre–re-expansion contraction (PRC) (**B**); mid–re-expansion contraction (MRC) (pumping or collapse) (**C**); and PRC and MRC (**E**). Ai = initial blastocyst area; Af = final blastocyst area; A1 = blastocyst area at re-expansion beginning; A2 = blastocyst area at re-expansion ending.

Conversa. Contractions of vitrified blastocysts. Fertil Steril 2026.

On day 5 or 6, 5–8 TE cells opposite the ICM were biopsied with a pipette by pulling or flicking (34). Chromosomal analysis was performed via next-generation sequencing (Thermo Fisher Scientific, Waltham, Massachusetts).

Embryo vitrification and transfer

Vitrification and warming were performed using Cryotop (Kitazato BioPharma, Fuji, Japan) (35). Warmed embryos were cultured in EmbryoScope incubators (37 °C, 5% CO_2, and 5% O_2) until transfer, scheduled 3–4 hours later. Embryos showing >50% degeneration without re-expansion after warming were deemed nonviable (n = 21). Transfers of vitrified-warmed embryos took place in modified natural or artificial cycles, with luteal support provided by 400 mg of vaginal progesterone (Progeffik; Lab. Effik, Meudon, France) every 12 hours. Implantation was confirmed by fetal heartbeat from the eighth week of pregnancy.

Statistical analysis

Univariate analyses of re-expansion and contraction parameters, AI and ASEBIR grades, and covariates (listed in Supplemental Table 1, available online) were performed using the Student *t*-test, chi-square test, and 1-way analysis of variance with post hoc test, as appropriate. Multivariate logistic regression analysis with forward procedure was applied to relevant variables to control for potential confounding factors. Results were considered statistically significant when $P < .05$. Area under the receiver operating curve (AUC-ROC) served to determine the performance of the predictive parameters. Statistical analyses were conducted using IBM Statistical Package for the Social Sciences (SPSS) 25.0 software (IBM Corp., Armonk, New York).

RESULTS

A total of 846 vitrified blastocysts were warmed, with a survival rate of 97.5%. The mean postwarming incubation time was 3.47 ± 0.84 hours. The positive fetal heartbeat rate was 46.1% for transferred embryos with known implantation data (n = 815), and LB rate was 40.3% (n = 799). Means, SDs, ranges, or frequencies for the characteristics of the study population are presented in Supplemental Table 1.

Among the clinical variables described, only cycle type and day of blastulation were associated with outcomes ($P<.05$), with natural cycles and day 5 blastocysts showing higher success rates than day 6 blastocysts. However, embryos from artificial cycles had better morphology, likely reflecting the patient profile: often of advanced maternal age (suboptimal endometrial conditions) and with donor oocytes. Preimplantation genetic testing for aneuploidies was not significantly related to clinical outcomes (LB rate of 39.4% for non-PGT-A vs. 44.5% for PGT-A, $P=.268$).

Postwarming re-expansion

Of the 846 warmed blastocysts, 38 (4.5%) did not start re-expansion after culture. Of the non–re-expanded embryos, 22 (57.9%) were transferred; however, their clinical success

TABLE 1

Descriptive analysis of re-expansion variables for positive and negative implantation and live birth outcomes.

Variable	Clinical outcome	Implantation n	Implantation Mean ± SD	Implantation *P* value	Live birth n	Live birth Mean ± SD	Live birth *P* value
Re-expansion duration (h)	-	815	3.14 ± 0.85	.024	799	3.15 ± 0.86	.004
	+		3.00 ± 0.85			2.97 ± 0.84	
Maximum thickness of the ZP (μm)	-	790	14.71 ± 3.93	.003	775	14.61 ± 3.92	.019
	+		13.90 ± 3.70			13.95 ± 3.72	
Minimum thickness of the ZP (μm)	-	784	11.88 ± 4.92	<.001	770	11.73 ± 4.99	.006
	+		10.61 ± 4.92			10.73 ± 4.85	
Initial blastocyst size (μm^2)	-	815	12,339 ± 3,407	.009	799	12,310 ± 3,405	.001
	+		12,993 ± 3,715			13,143 ± 3,816	
Final blastocyst size (μm^2)	-	815	18,963 ± 6,202	<.001	799	19,166 ± 6,237	.001
	+		20,826 ± 5,972			20,698 ± 5,965	
Blastocyst size at re-expansion beginning (μm^2)	-	815	11,003 ± 2,284	.026	799	10,989 ± 2,907	.008
	+		11,475 ± 3,147			11,573 ± 3,221	
Blastocyst size at re-expansion ending (μm^2)	-	815	19,411 ± 6,240	<.001	799	19,593 ± 6,271	.003
	+		21,044 ± 6,121			20,932 ± 6,131	
ZP thinning (μm)	-	784	2.83 ± 3.14	.060	770	2.88 ± 3.19	.188
	+		3.27 ± 3.31			3.19 ± 3.28	
Re-expansion size (μm^2)	-	815	8,408 ± 5,338	.002	799	8,604 ± 5,384	.051
	+		9,557 ± 5,193			9,350 ± 5,173	
ZP thinning speed (μm/h)	-	784	0.88 ± 1.00	.016	770	0.89 ± 1.01	.049
	+		1.06 ± 1.11			1.05 ± 1.10	
Re-expansion speed (μm^2/h)	-	815	2,681 ± 1,575	<.001	799	2,736 ± 1,570	<.001
	+		3,238 ± 1,637			3,209 ± 1,668	

Note: ZP = zona pellucida.

Conversa. Contractions of vitrified blastocysts. Fertil Steril 2026.

rate was 18.2%, significantly lower than those that re-expanded (implantation, 46.8% [P=.008]; LB, 40.9% [P=.032]). Postwarming incubation time was shorter in blastocysts that resulted in LB (3.36 ± 0.83 vs. 3.57 ± 1.17, P=.004). The descriptive data of all re-expansion parameters analyzed according to clinical outcomes are collected in Table 1. Initial blastocyst size and size at the beginning of re-expansion were different when a PRC occurred (48.7% of cases), as can be seen in Figure 2. On the other hand, final blastocyst size and size at the end of re-expansion were different when an MRC occurred right at the end of incubation (9.7%).

The duration of re-expansion and the maximum and minimum thickness of the ZP were lower in blastocysts with positive outcomes. On the other hand, initial and final blastocyst size, blastocyst size at the beginning and ending of re-expansion, re-expansion speed, and ZP thinning speed were positively correlated with implantation and LB. Re-expansion size was also higher in implanted embryos. However, ZP thinning was not related to either treatment outcome (Table 1).

Details of the analysis correlating PGT-A status with postwarming re-expansion are provided in Supplemental Table 2. None of the analyzed parameters were associated with clinical outcomes when assessing PGT-A embryos separately (all assisted-hatched and confirmed euploid), whereas the results for non-PGT-A embryos (not assisted-hatched and of unknown ploidy status) were similar to those observed in the overall population.

Other morphological features: ICM size and CSs

Other morphological variables such as the diameter of the ICM and the presence of CS between the mass and the TE were also analyzed. The ICM size (μm) was larger in blastocysts that successfully implanted (2,252.75 ± 760.95) or gave an LB (2,279.08 ± 781.18) than in those that did not (2,113.88 ± 677.08, P=.007; 2,101.90 ± 677.53, P=.001). The presence of CS was observed in 47.4% of the total population of embryos, and it was related to a higher implantation rate (50.5% vs. 43%, P=.033).

Logistic regression analyses including these two variables in addition to the re-expansion variables were performed to assess potentially predictive parameters and confounding factors. The models identified re-expansion speed, ICM area, and CS along with cycle type and day of blastulation as the most predictive variables for both clinical outcomes, together with re-expansion duration and final

TABLE 2

Results of the multivariate logistic regression analysis of tested parameters for implantation and live birth outcomes in transferred warmed embryos.

		Implantation		Live birth	
Variables in the equation		**OR[a]**	**95% CI**	**OR[a]**	**95% CI**
Re-expansion					
Final blastocyst size		—	—	1.08	1.02–1.13
Re-expansion size		—	—	1.15	1.07–1.24
Re-expansion speed		1.24	1.12–1.36	1.44	1.20–1.73
ICM area		1.30	1.06–1.59	1.30	1.05–1.61
Cytoplasmic strings (48.1%)		1.41	1.06–1.90	1.41	1.04–1.92
Type of cycle: natural (27.1%) vs. artificial (72.9%)		1.58	1.14–2.20	1.44	1.03–2.02
Day of blastulation: 5 (83.6%) vs. 6 (16.4%)		1.60	1.06–2.42	1.69	1.08–2.58
Re-expansion and contractions					
Final blastocyst size		—	—	1.08	1.02–1.13
Re-expansion size		—	—	1.15	1.07–1.24
Blastocyst size at re-expansion beginning		1.06	1.00–1.11	—	—
Re-expansion speed		1.21	1.10–1.34	1.44	1.20–1.73
ICM area		–	–	1.30	1.05–1.61
Cytoplasmic strings (48.1%)		1.50	1.11–2.03	1.41	1.04–1.92
Collapse		1.94	1.07–3.54	–	–
Type of cycle: natural (27.1%) vs. artificial (72.9%)		1.59	1.15–2.22	1.44	1.03–2.02
Day of blastulation: 5 (83.6%) vs. 6 (16.4%)		—	—	1.69	1.08–2.58
Re-expansion, contractions, and morphology					
Postwarming ASEBIR	B (69.0%) vs. C (15.2%)	3.22	2.01–5.17	3.42	2.02–5.78
morphology	A (15.9%) vs. C (15.2%)	2.95	1.65–5.27	2.69	1.41–5.13
Last postwarming AI score		—	—	1.19	1.04–1.36
Re-expansion speed		1.19	1.08–1.32	1.38	1.15–1.65
Re-expansion size		—	—	1.09	1.03–1.15
ICM area		1.30	1.05–1.59	1.37	1.11–1.69
Cytoplasmic strings (48.1%)		1.41	1.05–1.90	—	—
Type of cycle: natural (27.1%) vs. artificial (72.9%)		1.64	1.17–2.29	1.54	1.09–2.17

Note: Each model included the variables listed in each section, discarding the others that were not significant. ASEBIR = Spanish Association for the Study of Reproductive Biology; CI = confidence intervals; ICM = inner cell mass; OR = odds ratio.

[a] ORs computed from stepwise multivariate logistic regression.

Conversa. Contractions of vitrified blastocysts. Fertil Steril 2026.

blastocyst size for LB (Table 2). The models' performance achieved AUC-ROC values of 0.623 for implantation and 0.648 for LB.

Postwarming contractions: PRC, pumping and collapse

Of the total population of warmed blastocysts (n = 846), 64.1% underwent some contraction during postwarming incubation. Contraction before initiating re-expansion (PRC) was observed in 48.7% embryos, whereas 20.9% contracted midway through re-expansion (MRC) (Video 2).

The implantation rate (n = 815) was significantly higher in embryos with PRC (50.0%) than in those without (42.1%, $P=.024$); however, no correlation was found in the shrinkage percentage. The presence and number of MRCs were not related to outcome; however, their shrinkage percentage was significantly lower in blastocysts that implanted (12.27% [95% confidence interval, 9.28–15.26]) than in those that did not (17.49% [95% confidence interval, 14.10–20.89], $P=.027$).

Considering these confidence intervals, we established a threshold to differentiate MRCs between weak contractions or "pumping" (<15% shrinkage) and strong contractions or "collapse" (>15% shrinkage). Pumping occurred in 14.4% of total blastocysts (n = 846), and collapse occurred in 8.4%. Pumping embryos had slightly but not significantly higher implantation and LB rates (50.0% and 42.5, respectively) than nonpumping ones (45.3% and 39.9%); however, the presence of collapse reduced the implantation rate from 47.3% to 31.8% ($P=.016$) and the LB rate from 41.5% to 27.3% ($P=.024$).

Postwarming incubation time was longer in embryos with collapse (4.37 ± 3.05 vs. 3.61 ± 2.54, $P=.017$); however, it was not related to pumping.

More PGT-A embryos presented pumping (26.4% vs. 12.1%, $P<.001$) and had less incidence of PRC (17.1% vs. 55.0%, $P<.001$) compared with non-PGT-A embryos. No significant difference between the groups was observed in the case of collapse (it is noted that PGT-A embryos with collapse were n = 14). Contractions were not associated with clinical outcomes among PGT-A embryos, whereas non-PGT-A embryos showed results similar to the overall population.

Moreover, embryos not artificially hatched before vitrification (n = 706) were able to hatch naturally after warming more easily if they had pumped (18.8%) than if not (8.7%, $P = .003$). Natural hatching was less likely in collapsed embryos (2.9%) compared with that in noncollapsed ones (8.8%), although not significantly.

We conducted logistic regression models as described earlier but incorporating the identified significant variables related to the presence of PRCs, the shrinkage percentage of MRCs, and the occurrence of pumping and collapse. Variables predictive for implantation were blastocyst size at re-expansion beginning, re-expansion speed, CS, presence of collapse, and type of cycle (area under the curve, 0.641), whereas for LB outcome, the same variables as in the previous section remained predictive, displacing the parameters related to contractions out of the model (Table 2).

Correlation between postwarming contractions and conventional and AI morphological assessments

Previtrification and postvitrification ASEBIR (Supplemental Table 3) and AI scores (Supplemental Table 4) were significantly correlated with clinical outcomes. Because ASEBIR categories A and B were similar, they were pooled and stratified using the global medians of the AI scores, yielding three distinct groups (C, A^-/B^-, and A^+/B^+) with significantly different clinical outcomes (Supplemental Table 5).

Pre–re-expansion contraction was more frequent in warmed embryos with better previtrification (A, 62.1%; B, 49.4%; C, 32.6%; $P<.001$) and postwarming (A, 60.5%; B, 50.2%; C, 35.6%; D, 17.6%; $P<.001$) ASEBIR qualities and with higher previtrification (n = 694; PRC, 4.30 ± 1.72, vs. no PRC, 3.35 ± 1.73; $P<.001$) and first postwarming (n = 838; no PRC, 1.66 ± 0.89, vs. PRC, 1.88 ± 0.99; $P=.001$) AI scores.

The AI score was higher when evaluating first postwarming incubation image in embryos that pumped (0.19 ± 0.12) than in those that not (0.17 ± 0.09, $P=.035$). On the other hand, blastocysts that suffered collapse received worse pre-ASEBIR (A, 5.6%; B, 7.1%; C, 17.1%; $P=.001$) and post-ASEBIR (A, 4%; B, 7.4%; C, 15.6%; D, 18.8%; $P=.002$) classifications and lower prewarming (collapse, 0.33 ± 0.20, vs. no collapse, 0.39 ± 0.18; $P=.025$) and last postwarming (collapse, 0.19 ± 0.12, vs. no collapse, 0.29 ± 0.13; $P<.001$) postwarming AI scores.

When adding the ASEBIR and AI scores to the logistic regression analysis, the model identified postwarming ASEBIR morphology, re-expansion speed, ICM area, and cycle type as the most relevant variables for predicting implantation and LB (Table 2). Cytoplasmic strings also predicted implantation, whereas last postwarming AI score and re-expansion size were predictive for LB. The models achieved AUC-ROC values of 0.647 for implantation and 0.663 for LB.

DISCUSSION

The findings of this study underscore the critical role of blastocyst re-expansion after vitrification and warming in pregnancy success. For the first time, we propose new markers of blastocyst viability influenced by the vitrification/warming process.

Our results demonstrate that a small percentage of blastocysts (4.5%) fail to initiate re-expansion after culture and that these embryos had significantly lower LB rate (18.2%) than those that did re-expand (40.9%). This study agrees with previous research on the association between re-expansion dynamics and clinical outcomes, suggesting that faster re-expansion and a thinner ZP enhance the likelihood of successful implantation (6,10–16). However, ZP thinning itself does not directly predict treatment outcomes, potentially because many embryos collapse during vitrification, resulting in an already thinned ZP at the

beginning of re-expansion because these embryos were expanded before vitrification.

Conversely, ICM size was positively correlated with success in pregnancy, consistent with findings of other studies (36–38). Although estimating ICM size from a 2-dimensional image represents a limitation, it serves as a close proxy for assessing its true volume. Cytoplasmic strings have recently been identified because they are a dynamic structure and could only be detected when embryonic development began to be recorded in time-lapse systems. Their function could be cellular communication between the ICM and TE through nutrient and signal transport (39). Joo et al. (39) and Ma et al. (40) reported CS in 81.20% and 79.08% of fresh blastocysts, respectively, whereas our study in vitrified-warmed embryos detected them in 47.4% of the total blastocysts. This lower percentage may be attributed to the inclusion of nonviable and non–re-expanded blastocysts, where CS identification was not possible. The presence of CS between ICM and TE was associated with implantation ($P<.05$), aligning with previous studies that identified CS as positive predictors of clinical pregnancy and LB (39, 40).

When an embryo is warmed, it may initially undergo a PRC. This shrinkage is a physiological response because of the widening of intercellular spaces between TE cells (5, 9). Trophectoderm cells are flaccid and pliable before this initial contraction, and as they reseal and start absorbing water, they become turgid, and re-expansion begins. On the basis of our results, the presence of PRC has been significantly associated with higher implantation rate ($P<.05$), suggesting that it may represent an attempt to release cryoprotectants before recovery of physiological cytoplasmic composition.

The lack of standardized definitions for "pumping" and "collapse," and the distinction between them, complicates cross-study comparisons and renders them imprecise and inconclusive. Although many investigators define collapse as a separation of TE from ZP (19, 20, 22), this may not accurately measure the magnitude of shrinkage. Moreover, time-lapse systems, which do not permit manual embryo rotation, introduce variability because of the fixed perspective of the observer and the collapsed embryo within the ZP. Other studies define collapse as a $\geq$50% reduction in volume, yet the clinical impact of contractions <50% remains underexplored (41). To better assess embryo quality, it is necessary to establish a clinically relevant threshold for volume reduction, which may differ between fresh and vitrified-warmed embryos. In our study, we defined the threshold between pumping and collapse as a 15% reduction in blastocyst volume, on the basis of confidence intervals for implanted and nonimplanted embryos. Niimura et al. (18) set a similar limit at 20%.

Our analysis of MRCs found that only strong contractions (>15% shrinkage) were correlated with reduced implantation and LB potential ($P<.05$). These collapses may indicate incomplete resealing of intercellular spaces, leading to re-expansion difficulties and implantation failure. In contrast, pumping or contractions <15% during re-expansion are likely normal and facilitate hatching, as observed in this and other studies (18).

The PGT-A/non–PGT-A variable showed no correlation with implantation or LB outcomes; however, we aimed to clarify any potential impact on postwarming dynamics because all PGT-A-tested embryos were assisted-hatched and euploid. These blastocysts showed higher ZP thickness, re-expansion size, and speed, likely because the ZP was breached and no longer exerted compressive pressure, allowing the TE to expand more freely and rapidly. The presence of pumping was also more frequent in PGT-A blastocysts, possibly because of the euploid status of these embryos or because of assisted hatching. Future research should focus on investigating aneuploid embryos using time-lapse systems after vitrification to determine whether pumping is associated with zona breakage (if ploidy is not related to pumping) or if it is correlated with euploid status, potentially facilitating hatching. Conversely, we found a significant negative correlation of PGT-A with PRC and initial and re-expansion beginning blastocyst sizes, possibly because direct exposure of the TE to cryoprotectants leads to more complete shrinkage during vitrification, so PGT-A blastocysts are already shrunken when warmed. None of the postwarming variables were related to clinical outcomes when analyzing PGT-A embryos solely, perhaps because of the low sample size (n = 140).

According to our results, the optimal postwarming incubation time to allow proper re-expansion could be 3 hours, not exceeding 3.5 hours, as lower LB rates and increased collapse have been observed at longer times.

Current conventional and AI-based embryo assessments have been correlated with postwarming blastocyst contractions, so their deeper understanding could enhance embryo selection. Our findings suggest that AI refines selection by distinguishing subgroups within different good-quality ASEBIR categories (A and B), providing additional discriminatory power for predicting outcomes. Training AI models specifically on postwarming images and integrating contraction detection into AI algorithms may improve the accuracy of pregnancy predictions in frozen cycles.

This study has some potential limitations, such as missing data on blastocysts with unknown clinical outcomes or low-quality images, low sample size of events such as collapse, generalizability, and unmeasured confounding factors.

Identifying new markers of blastocyst viability after warming enables better evaluation of how changes in vitrification and warming protocols impact survival. Specifically, this knowledge can help assess the effects of ultrafast vitrification and warming, guiding protocol refinements or culture adjustments to minimize adverse outcomes and enhance clinical success.

CONCLUSION

Understanding postvitrification warming contractions is essential for embryologists in assessing embryo viability. Specifically, collapses negatively affect implantation and LB potential, whereas pumping facilitates hatching. Faster re-expansion, PRC presence, and CS improve implantation outcome. Monitoring of these dynamics may assist in

determining whether an additional embryo should be warmed, ultimately improving the chances of achieving an LB.

Acknowledgments

The authors thank the embryologists and technicians of the IVF Laboratory from IVI-RMA Global Valencia for their clinical support and the Alife Health team for allowing us to test the AI software. This research has been funded by a grant from the Regional Ministry of Innovation, Universities, Science and Digital Society of the Valencian Community (Valencia, Spain) (CIACIF/2021/019), and by Spanish Ministry of Science and Innovation (Madrid, Spain) (CDTI-IDI-20240634).

CRediT Authorship Contribution Statement

Laura Conversa: Writing – original draft, Methodology, Investigation, Formal analysis, Data curation, Conceptualization. **Carla Giménez-Rodríguez:** Writing – review & editing, Data curation. **Lucía Murria:** Writing – review & editing, Formal analysis. **Lucía Alegre:** Writing – review & editing, Investigation. **Ana Cobo:** Writing – review & editing, Supervision. **Marcos Meseguer:** Writing – review & editing, Supervision, Methodology, Conceptualization.

Declaration of Interests

L.C. has nothing to disclose. C.G.-R. has nothing to disclose. L.M. has nothing to disclose. L.A. has nothing to disclose. A. C. has nothing to disclose. M.M. reports honoraria from Merck, Gideon Richter, Vitrolife, Genea Biomedx, MSD, Life Whisperer, Ferring, Theramex, and AIVF.

SUPPLEMENTAL MATERIAL

Supplemental data for this article can be found online at https://doi.org/10.1016/j.fertnstert.2025.10.013.

REFERENCES

1. Zeilmaker GH, Alberda AT, van Gent I, Rijkmans CM, Drogendijk AC. Two pregnancies following transfer of intact frozen-thawed embryos. Fertil Steril 1984;42:293–6.
2. Rall WF, Fahy GM. Ice-free cryopreservation of mouse embryos at -196 degrees C by vitrification. Nature 1985;313:573–5.
3. European IVF Monitoring Consortium (EIM) for the European Society of Human Reproduction and Embryology (ESHRE), Smeenk J, Wyns C, De Geyter C, Kupka M, Bergh C, et al. ART in Europe, 2019: results generated from European registries by ESHRE†. Hum Reprod 2023;38:2321–38.
4. Liebermann J. Vitrification: a simple and successful method for cryostorage of human blastocysts. Methods Mol Biol 2021;2180:501–15.
5. Hwang JY, Park JK, Kim TH, Eum JH, Song H, Kim JY, et al. The impact of post-warming culture duration on clinical outcomes of vitrified-warmed single blastocyst transfer cycles. Clin Exp Reprod Med 2020;47:312–8.
6. Fabian D, Gjørret JO, Berthelot F, Martinat-Botté F, Maddox-Hyttel P. Ultrastructure and cell death of in vivo derived and vitrified porcine blastocysts. Mol Reprod Dev 2005;70:155–65.
7. Biggers JD, Bell JE, Benos DJ. Mammalian blastocyst: transport functions in a developing epithelium. Am J Physiol 1988;255:C419–32.
8. Barcroft LC, Offenberg H, Thomsen P, Watson AJ. Aquaporin proteins in murine trophectoderm mediate transepithelial water movements during cavitation. Dev Biol 2003;256:342–54.
9. Magnuson T, Jacobson JB, Stackpole CW. Relationship between intercellular permeability and junction organization in the preimplantation mouse embryo. Dev Biol 1978;67:214–24.
10. Shu Y, Watt J, Gebhardt J, Dasig J, Appling J, Behr B. The value of fast blastocoele re-expansion in the selection of a viable thawed blastocyst for transfer. Fertil Steril 2009;91:401–6.
11. Desai N, Ploskonka S, Goodman L, Attaran M, Goldberg JM, Austin C, et al. Delayed blastulation, multinucleation, and expansion grade are independently associated with live-birth rates in frozen blastocyst transfer cycles. Fertil Steril 2016;106:1370–8.
12. Du QY, Wang EY, Huang Y, Guo XY, Xiong YJ, Yu YP, et al. Blastocoele expansion degree predicts live birth after single blastocyst transfer for fresh and vitrified/warmed single blastocyst transfer cycles. Fertil Steril 2016;105:910–9.e1.
13. Yin H, Jiang H, He R, Wang C, Zhu J, Li Y. The effects of blastocyst morphological score and blastocoele re-expansion speed after warming on pregnancy outcomes. Clin Exp Reprod Med 2016;43:31–7.
14. Coello A, Meseguer M, Galán A, Alegre L, Remohı J, Cobo A. Analysis of the morphological dynamics of blastocysts after vitrification/warming: defining new predictive variables of implantation. Fertil Steril 2017;108:659–66.e4.
15. Ebner T, Oppelt P, Radler E, Allerstorfer C, Habelsberger A, Mayer RB, et al. Morphokinetics of vitrified and warmed blastocysts predicts implantation potential. J Assist Reprod Genet 2017;34:239–44.
16. Hershko-Klement A, Raviv S, Nemerovsky L, Rom T, Itskovich A, Bakhshi D, et al. Standardization of post-vitrification human blastocyst expansion as a tool for implantation prediction. J Clin Med 2022;11:2673.
17. Lewis WH, Gregory PW. Cinematographs of living developing rabbit-eggs. Science 1929;69:226–9.
18. Niimura S. Time-lapse videomicrographic analyses of contractions in mouse blastocysts. J Reprod Dev 2003;49:413–23.
19. Marcos J, Pérez-Albalá S, Mifsud A, Molla M, Landeras J, Meseguer M. Collapse of blastocysts is strongly related to lower implantation success: a time-lapse study. Hum Reprod 2015;30:2501–8.
20. Viñals-Gonzalez X, Odia R, Cawood S, Gaunt M, Saab W, Seshadri S, et al. Contraction behaviour reduces embryo competence in high-quality euploid blastocysts. J Assist Reprod Genet 2018;35:1509–17.
21. Gazzo E, Peña F, Valdéz F, Chung A, Velit M, Ascenzo M, et al. Blastocyst contractions are strongly related with aneuploidy, lower implantation rates, and slow-cleaving embryos: a time lapse study. JBRA Assist Reprod 2020;24:77–81.
22. Cimadomo D, Marconetto A, Trio S, Chiappetta V, Innocenti F, Albricci L, et al. Human blastocyst spontaneous collapse is associated with worse morphological quality and higher degeneration and aneuploidy rates: a comprehensive analysis standardized through artificial intelligence. Hum Reprod 2022;37:2291–306.
23. Bodri D, Sugimoto T, Yao Serna J, Kawachiya S, Kato R, Matsumoto T. Blastocyst collapse is not an independent predictor of reduced live birth: a time-lapse study. Fertil Steril 2016;105:1476–83.e3.
24. Shimoda Y, Kumagai J, Anzai M, Kabashima K, Togashi K, Miura Y, et al. Time-lapse monitoring reveals that vitrification increases the frequency of contraction during the pre-hatching stage in mouse embryos. J Reprod Dev 2016;62:187–93.
25. Maezawa T, Yamanaka M, Hashimoto S, Amo A, Ohgaki A, Nakaoka Y, et al. Possible selection of viable human blastocysts after vitrification by monitoring morphological changes. J Assist Reprod Genet 2014;31:1099–104.
26. Conversa L, Bori L, Insua F, Marqueño S, Cobo A, Meseguer M. Testing an artificial intelligence algorithm to predict fetal heartbeat of vitrified-warmed blastocysts from a single image: predictive ability in different settings. Hum Reprod 2024;39:2240–8.
27. Loewke K, Cho JH, Brumar CD, Maeder-York P, Barash O, Malmsten JE, et al. Characterization of an artificial intelligence model for ranking static images of blastocyst stage embryos. Fertil Steril 2022;117:528–35.
28. Bori L, Meseguer F, Valera MA, Galan A, Remohi J, Meseguer M. The higher the score, the better the clinical outcome: retrospective evaluation of automatic embryo grading as a support tool for embryo selection in IVF laboratories. Hum Reprod 2022;37:1148–60.

29. Cerrillo M, Herrero L, Guillén A, Mayoral M, García-Velasco JA. Impact of endometrial preparation protocols for frozen embryo transfer on live birth rates. Rambam Maimonides Med J 2017;8:e0020.
30. Bellver J, Del Arco A, Pellicer A, Caracena L, Serra V, Labarta E, et al. Risk of preeclampsia and other pregnancy complications in frozen single euploid embryo transfers after natural versus artificial endometrial preparation: a truncated randomized controlled trial. Placenta 2025;163:1–7.
31. Valera MÁ, Garg A, Bori L, Meseguer F, de Los Santos JM, Meseguer M. Undisturbed culture: a clinical examination of this culture strategy on embryo in vitro development and clinical outcomes. Fertil Steril 2024;122:1037–47.
32. Cuevas-Saiz I, Pons MC, Cuadros M, Delgado A, Rives N, Moragas M, et al. The Embryology Interest Group: updating ASEBIR's morphological scoring system for early embryos, morulae and blastocysts. Med Reprod Embriol Clin 2018;5:42–54.
33. Bori L, Toschi M, Esteve R, Delgado A, Pellicer A, Meseguer M. External validation of a fully automated evaluation tool: a retrospective analysis of 68,471 scored embryos. Fertil Steril 2025;123:634–43.
34. Nohales M, Coello A, Martin A, Insua F, Meseguer M, de Los Santos MJ. Should embryo rebiopsy be considered a regular strategy to increase the number of embryos available for transfer? J Assist Reprod Genet 2023;40:1905–13.
35. Cobo A, de los Santos MJ, Castellò D, Gámiz P, Campos P, Remohí J. Outcomes of vitrified early cleavage-stage and blastocyst-stage embryos in a cryopreservation program: evaluation of 3,150 warming cycles. Fertil Steril 2012;98:1138–11346.e1.
36. Almagor M, Harir Y, Fieldust S, Or Y, Shoham Z. Ratio between inner cell mass diameter and blastocyst diameter is correlated with successful pregnancy outcomes of single blastocyst transfers. Fertil Steril 2016;106:1386–91.
37. Shapiro BS, Richter KS, Harris DC, Daneshmand ST. Optimal inner cell mass size and shape for a human blastocyst. Fertil Steril 2000;74:S43.
38. Richter KS, Harris DC, Daneshmand ST, Shapiro BS. Quantitative grading of a human blastocyst: optimal inner cell mass size and shape. Fertil Steril 2001;76:1157–67.
39. Joo K, Nemes A, Dudas B, Berkes-Bara E, Murber A, Urbancsek J, et al. The importance of cytoplasmic strings during early human embryonic development. Front Cell Dev Biol 2023;11:1177279.
40. Ma BX, Yang L, Tian Y, Jin L, Huang B. Cytoplasmic strings between ICM and mTE are a positive predictor of clinical pregnancy and live birth outcomes: a time-lapse study. Front Med (Lausanne) 2022;9:934327.
41. Sciorio R, Herrer Saura R, Thong KJ, Esbert Algam M, Pickering SJ, Meseguer M. Blastocyst collapse as an embryo marker of low implantation potential: a time-lapse multicentre study. Zygote 2020:1–9.

Dinámica de reexpansión y contracción después del calentamiento de blastocistos vitrificados: la magnitud y el momento de la contracción están correlacionados con el resultado del embarazo.

Objetivo: Analizar la relación entre la dinámica de los blastocistos después del calentamiento, específicamente la re-expansión y las contracciones, con las tasas de implantación y de nacimiento vivo (LB), así como con la viabilidad embrionaria global tras la vitrificación y el calentamiento.

Diseño: Estudio de cohorte retrospectivo.

Entorno: Centro privado de fertilización in vitro afiliado a una universidad.

Sujetos: Un total de 846 blastocistos calentados procedentes de pacientes sometidas a ciclos con embriones congelados (febrero de 2022 a mayo de 2024).

Intervención: Ninguna.

Medidas principales de resultado: Se analizaron las dinámicas de re-expansión tras el calentamiento y los tipos de contracción —contracciones previas a la re-expansión (PRCs) y contracciones durante la re-expansión (MRCs) (tipo "pumping" o colapso)—, el tamaño de la masa celular interna y las cuerdas citoplasmáticas (CSs), evaluando su correlación con las tasas de implantación y de nacido vivo. Además, los modelos de regresión logística incorporaron estas variables junto con evaluaciones convencionales de la calidad embrionaria y evaluaciones basadas en inteligencia artificial (AI).

Resultados: De los 846 blastocistos vitrificados, el 97,5% sobrevivió al calentamiento, de los cuales el 95,5% pudo iniciar la re-expansión. Las tasas de implantación y de nacido vivo fueron mayores (46,8% y 46,9%, respectivamente) en los blastocistos que se re-expandieron frente a los que no lo hicieron (18,2% para ambos resultados).
Una mayor velocidad de re-expansión, una zona pelúcida más delgada, un mayor tamaño final del blastocisto y una mayor área de la masa celular interna se correlacionaron positivamente con el éxito del tratamiento.
Además, se identificaron CSs en el 47,4% de los embriones, asociándose con una mayor tasa de implantación (50,5% frente a 43%). La presencia de PRCs se asoció con tasas de implantación más altas (50% frente a 42,1%). En cambio, la presencia de colapso (contracción MRC con reducción >15%) redujo las tasas de implantación (de 47,3% a 31,8%) y de nacimiento vivo (de 41,5% a 27,3%).
Los embriones con pumping (contracción MRC con reducción <15%) tuvieron mayor probabilidad de eclosionar de forma natural tras el calentamiento (18,8% frente a 8,7%). Las contracciones tras el calentamiento se correlacionaron con la calidad morfológica embrionaria evaluada tanto por embriólogos como por un software de IA basado en imágenes.

Conclusión: La dinámica de re-expansión y contracción tras el calentamiento constituye un indicador crítico de la viabilidad y competencia embrionaria. En particular, las MRCs intensas o colapsos afectan negativamente al potencial de implantación y de nacimiento vivo, mientras que contracciones leves o el fenómeno de pumping pueden favorecer una eclosión exitosa.
Una re-expansión más rápida, la presencia de PRC y la presencia de cuerdas citoplasmáticas (CS) mejoran el resultado de implantación, lo que sugiere la necesidad de tener en cuenta estos parámetros al evaluar embriones calentados e integrar las métricas de contracción en los sistemas de selección embrionaria asistidos por inteligencia artificial (IA).
Por lo tanto, un seguimiento más detallado de estas dinámicas podría orientar la selección embrionaria y la toma de decisiones clínicas, optimizando las tasas de éxito del embarazo.